

# Differences in cumulus cell gene expression indicate the benefit of a pre-maturation step to improve *in-vitro* bovine embryo production

Cecilia Dieci<sup>1,†</sup>, Valentina Lodde<sup>1,†</sup>, Rémi Labreque<sup>2</sup>, Isabelle Dufort<sup>2</sup>, Irene Tessaro<sup>1,3</sup>, Marc-André Sirard<sup>2</sup>, and Alberto M. Luciano<sup>1,\*</sup>

<sup>1</sup>Reproductive and Developmental Biology Laboratory, Department of Health, Animal Science and Food Safety, University of Milan, Via Celoria 10, 20133 Milan, Italy <sup>2</sup>Centre de Recherche en Biologie de la Reproduction, Département des Sciences Animales, Université Laval, 2440, boulevard Hochelaga, Québec, (Québec) G1V 0A6, Canada <sup>3</sup>Present address: I.R.C.C.S. Istituto Ortopedico Galeazzi, Via R. Galeazzi, 4, 20161 Milan, Italy

\*Correspondence address. Dipartimento di Scienze Veterinarie per la Salute, la Produzione Animale e la Sicurezza Alimentare, Università degli Studi di Milano, Via Celoria, 10, 20133 Milano, Italy. E-mail: alberto.luciano@unimi.it

Submitted on May 5, 2016; resubmitted on July 21, 2016; editorial decision August 19, 2016; accepted on August 20, 2016

**STUDY QUESTION:** Does the gene expression profile of cumulus cells (CC) accompanying oocytes with different degrees of chromatin compaction within the germinal vesicle (GV) reflect the oocyte's quality and response in culture during *in-vitro* embryo production (IVP).

**SUMMARY ANSWER:** The transcriptomic profile of the CC is related to oocyte competence, setting the stage for the development of customized pre-maturation strategies to improve IVP.

**WHAT IS KNOWN ALREADY:** Oocytes complete the acquisition of their competence during antral follicle development. During this period, the chromatin configuration within the GV changes dynamically and is indicative of oocyte's developmental potential. The interactions between somatic and germ cells modulate chromatin morphology and function and are critical for acquisition of oocyte competence.

**STUDY DESIGN, SIZE, DURATION:** Bovine cumulus–oocyte complexes (COC) were isolated from 0.5 to 6 mm antral follicles. Surrounding CC were separated from the oocyte and classified as GV0, GV1, GV2 and GV3 according to the degree of the oocyte's chromatin compaction.

**PARTICIPANTS/MATERIALS, SETTING, METHOD:** RNA extracted from CC of each group was amplified and hybridized on a bovine embryo-specific 44 K Agilent slide. The CC\_GV1, CC\_GV2 and CC\_GV3 classes were each hybridized against the CC\_GV0 class, representing an early oocyte differentiation stage with poor development competence. The data were normalized and fold changes of the differentially expressed genes were determined. Microarray data were validated using quantitative RT-PCR on selected targets. Microarray data were further analyzed through: (i) between-group analysis (BGA), which classifies the samples according to their transcriptomic profiles; (ii) cluster analysis according to the expression profile of each gene; and (iii) Ingenuity Pathway Analysis (IPA) to study gene regulation patterns and predicted functions. Furthermore, CC of each GV group were cultured and apoptotic cells were assessed after 3 h by caspase analysis. Finally, based on the analysis of CC transcriptomic profiles and the relationship between morphological features of the COC and the oocyte chromatin configuration, a customized, stage-dependent oocyte pre-maturation (pre-IVM) system was used to improve oocyte developmental potential before IVM. For this, the blastocyst rate and quality were assessed after *in-vitro* maturation and fertilization of pre-matured oocytes.

**MAIN RESULTS AND THE ROLE OF CHANCE:** Overall, quantitative RT-PCR results of a subset of five selected genes were consistent with the microarray data. Clustering analysis generated 16 clusters representing the main profiles of transcription modulation. Of the 5571 significantly differentially expressed probes, the majority (25.49%) best fitted with cluster #6 (downregulation between CC\_GV0 and CC\_GV1 and stable low levels in successive groups). IPA identified the most relevant functions associated with each cluster. Genes included in cluster #1 were mostly related to biological processes such as 'cell cycle' and 'cell death and survival', whereas genes included in cluster #5 were mostly related to 'gene expression'. Interestingly, 'lipid metabolism' was the most significant function identified in clusters #6, #9 and

<sup>†</sup> Contributed equally.

#12. IPA of gene lists obtained from each contrast (i.e., CC\_GV0 vs. CC\_GV1; CC\_GV0 vs. CC\_GV2; CC\_GV0 vs. CC\_GV3) revealed that the main affected function in each contrast was 'cell death and survival'. Importantly, apoptosis was predicted to be inhibited in CC\_GV1 and CC\_GV2, but activated in CC\_GV3. Caspase analysis indicated that a low percentage of CC\_GV0 was prone to undergo apoptosis but apoptosis increased significantly in CC from oocytes with condensed chromatin, reaching a peak in CC\_GV3 ( $P < 0.05$ ). Finally, the tailored oocyte pre-maturation strategy, based on morphological features of the COC and the oocyte chromatin configuration, demonstrated that pre-IVM improved the developmental capability of oocytes at early stages of differentiation (GV1-enriched COC) but was detrimental for oocytes at more advanced stages of development (GV2 and GV3-enriched COC).

**LARGE SCALE DATA:** The data are available through the GEO series accession number GSE79886.

**LIMITATIONS, REASONS FOR CAUTION:** This study was conducted with bovine samples. Whether or not the results are applicable to human oocytes requests further elucidation. Embryo transfer experiments are required to determine whether the improvement in blastocyst rates in the tailored system leads to increased live birth rates.

**WIDER IMPLICATIONS OF THE FINDINGS:** The identification of multiple non-invasive biomarkers predictive of oocyte quality can greatly strengthen the pre-IVM approach aimed to improve IVM outcomes. These results have potentially important implications in treating human infertility and in developing breeding schemes for domestic mammals.

**STUDY FUNDING/COMPETING INTEREST(S):** This work was supported in part by NSERC Strategic Network EmbryoGENE, Canada and in part by CIG—Marie Curie Actions—Reintegration Grants within the EU 7FP (n. 303640, 'Pro-Ovum'). The authors declare no potential conflict of interest.

**Key words:** oocyte / chromatin / follicle / granulosa cells / cumulus cells / apoptosis / pre-maturation / embryo development

## Introduction

*In-vitro* embryo production (IVP) remains inefficient in both clinical applications of human reproduction and animal breeding. In particular, the development of suitable conditions for *in-vitro* oocyte maturation (IVM) that supports high quality oocyte production is a major challenge in assisted reproductive technologies (Smitz *et al.*, 2011). In the bovine, although many attempts to increase the number of transferable embryos have been made in recent decades, the efficiency of IVP techniques, calculated as the proportion of immature oocytes aspirated from middle antral follicles (2–8 mm in diameter) that reach the blastocyst stage of embryonic development, is struggling to overcome a 35% threshold (Lonergan and Fair, 2008), unless very specific hormonal programming is used, that can double this rate (Blondin *et al.*, 2002; Nivet *et al.*, 2012; Landry *et al.*, 2016). In fact, oocytes retrieved from non-treated animals reveal heterogeneous cellular and molecular features as well as distinct embryonic developmental capabilities (Pavlok *et al.*, 1992; Blondin and Sirard, 1995). On the other hand, it is well known that oocytes enclosed in early antral follicles (<2 mm in diameter) have not yet acquired the competence to spontaneously resume meiosis once isolated from the follicular compartment (Pavlok *et al.*, 1992; Blondin and Sirard, 1995); thus, they are generally not used in standard IVP protocols.

The diversity of oocyte competence is mainly due to the intrinsic heterogeneity of the cohort of follicles from which cumulus–oocyte complexes (COC), to be subjected to standard IVP procedures, are isolated (Merton *et al.*, 2003; Vassena *et al.*, 2003). In cows, as in humans, only one oocyte is released at each reproductive cycle while the remaining follicles undergo atresia (Gougeon, 1986; Lussier *et al.*, 1987). It is widely accepted that one of the main factors that impairs oocyte ability to become an embryo *in vitro* is the precocious meiotic resumption that occurs when oocytes are isolated from the follicles. This, indeed, interrupts the process of oocyte capacitation

(Hyttel *et al.*, 1997; Gilchrist *et al.*, 2008; Coticchio *et al.*, 2015) and creates an asynchrony between the nuclear and the cytoplasmic events that are required for oocyte differentiation program before ovulation (Eppig *et al.*, 1994). In addition, a large proportion of these oocytes have already started an atretic process (Gougeon, 1996; Adams *et al.*, 2008; Monniaux *et al.*, 2014).

Oocyte quality heterogeneity is reflected in differences in the large-scale configuration of the chromatin enclosed in the germinal vesicle (GV) of immature oocytes (reviewed in Zuccotti *et al.*, 2005; De La Fuente, 2006; Luciano and Lodde, 2013; Luciano *et al.*, 2014). In cows, oocytes isolated from early to middle antral follicles have four different patterns of chromatin configuration, from GV0 to GV3, which are characterized by progressive increases in chromatin compaction (Lodde *et al.*, 2007), transcriptional silencing (Lodde *et al.*, 2008; Luciano *et al.*, 2011) and global DNA methylation (Lodde *et al.*, 2009). Notably, oocytes with a GV0 configuration (isolated from early antral follicles) display a very limited capability to resume meiosis, while virtually all of the GV1, GV2 and GV3 oocytes (isolated from mid-antral follicles) are capable of reaching the metaphase II (MII) stage *in vitro*, regardless their GV configuration (Lodde *et al.*, 2007). However, only a limited proportion of GV1 oocytes reach the blastocyst stage after IVF, while GV2 and GV3 oocytes have significantly higher embryonic developmental potentials (Lodde *et al.*, 2007). Thus, large-scale chromatin configuration is a marker of oocyte differentiation and competence.

It is clear that a better characterization of the molecular determinants of oocyte heterogeneity would be beneficial in understanding basic oocyte biology as well as in improving IVP efficiency. With this view, we have recently analyzed the transcriptomic profile of bovine oocytes with different chromatin configurations to identify changes in mRNA expression in the oocyte during the GV0-to-GV3 transition (Labrecque *et al.*, 2015). The present study aimed to expand this knowledge by assessing the transcriptomic profile of cumulus cells (CC) isolated from oocytes with different chromatin configurations. In

fact, proper assessment of the oocyte 'signature' cannot overlook features of the surrounding CC. It is well established that the CC play a fundamental role in the modulation of oocyte competence acquisition. During folliculogenesis, oocyte growth and differentiation rely upon the establishment of a microenvironment generated by bidirectional paracrine regulatory signals, and intercellular heterologous gap junction communications between oocytes and somatic cells are pivotal (Eppig, 2001; Matzuk et al., 2002; Gilchrist et al., 2008). Moreover, previous studies show that the tight association between oocyte and companion CC is required for the progressive suppression of transcriptional activity, chromatin remodeling and competence acquisition during the final phase of oocyte growth in mice (De La Fuente and Eppig, 2001), cows (Luciano et al., 2011) and humans (Sanchez et al., 2015).

Furthermore, based on the results of our microarray analysis, in a second part of this study, we hypothesize that each class of oocytes responds differently to the cultural environment during IVP. To test this hypothesis, and considering that it is technically not possible to identify the chromatin configuration without DNA staining after removal of CC, we first looked for possible morphological markers that could be related to the chromatin configuration of the corresponding oocyte, and used these criteria to select a population of COC enriched in GV1 oocytes (which are less competent compared with GV2 and GV3). Then, on the basis of the microarray results, we designed a culture system specifically formulated to fulfill the specific needs of the oocyte at a specific stage and to support *in-vitro* development. This system was used as proof-of-concept of an *in-vitro* differentiation strategy, the so-called 'pre-maturation' system, in order to improve oocyte developmental potential before IVM. This, in turn, confirmed the hypothesis that each class of oocytes responds differently to the cultural environment during IVP.

## Materials and Methods

All chemicals and reagents were purchased from Sigma-Aldrich, St. Louis, MO USA., unless otherwise stated.

### COC collection

Ovaries were recovered at the abattoir (INALCA Spa, Ospedaletto Lodigiano, LO, IT 2270 M CE, Italy) from 4 to 8 years old Holstein dairy cows and COC were retrieved from early (0.5–2 mm) and middle antral follicles (2–8 mm) as previously described (Lodde et al., 2007). All the COC collected were then washed in medium 199 (M199) supplemented with HEPES 20 mM, 1790 units/L Heparin and 0.4% of bovine serum albumin (HM199) and examined under a stereomicroscope. Only COC suitable for standard IVP procedures were used. Precisely, only oocytes medium-brown in color, with homogenous or finely granulated ooplasm and surrounded by five or more complete layers of CC were included in the study (Luciano et al., 2005). The same morphological selection criteria are commonly accepted by the scientific community and applied in the commercial settings worldwide (Gordon, 2003; Stringfellow and Givens, 2010).

### CC isolation

COC were individually vortexed (2 min, 35 Hz) in HM199 supplemented with 5% of calf serum (Gibco, Thermo Fisher Scientific, Waltham, MA USA) to isolate CC. In order to assess the chromatin configuration of oocytes corresponding to each cumulus, the denuded oocytes (DO) were individually washed in HM199, stained in HM199 containing 1 µg/ml

Hoechst 33342 for 5 min in the dark, and then transferred into a 5-µl drop of the same medium, overlaid with mineral oil and observed under an inverted fluorescence microscope (Olympus IX50, Olympus Italia S.r.l., Segrate, Italy, magnification ×40). Oocytes were classified according to the degree of chromatin compaction within the nuclear envelope as previously described (Lodde et al., 2007): the GV0 stage is characterized by a diffuse filamentous pattern of chromatin in the whole nuclear area; the GV1 and GV2 configurations represent early and intermediate stages, respectively, of chromatin remodeling, a process starting with the appearance of few foci of condensation in GV1 oocytes and proceeding with the formation of distinct clumps of condensed chromatin in GV2 oocytes; the GV3 is the stage where the maximum level of condensation is reached with chromatin organized into a single clump.

For transcriptomic and gene expression analyses, CC isolated from each COC were individually collected in RNase-free tubes, washed twice in cold PBS followed by centrifugation at 10.600 g for 1 min at 4°C. After the removal of the supernatant, CC pellets (in the minimum volume of PBS possible) were snap-frozen in liquid nitrogen and stored at –80°C until RNA extraction. For the assessment of pan-caspase activity, CC were isolated following the same experimental procedure with the exception that they were removed by pipetting to avoid cell damage. Then, CC isolated from a single COC were transferred into culture medium and assayed as described below.

### RNA extraction

Groups of CC isolated from 10 oocytes with the same chromatin configuration were pooled and processed for total RNA extraction. Total RNA was extracted and purified with the Pico-Pure RNA Isolation Kit (ARCTURUS®, Thermo Fisher Scientific) following the manufacturer's protocol, with minor modifications. Briefly, 10–30 µl of extraction buffer was added to each tube containing CC pellet from a single COC and incubated 30 min at 42°C. Following incubation, extraction reaction mixtures from 10 tubes with CC isolated from oocytes bearing the same chromatin configuration were pooled and equal volumes of EtOH 70% were added to each tube. Then, 250 µl of the RNA sample and EtOH mixture was loaded into the preconditioned purification columns and centrifuged for 2 min at 100g; this step was repeated until all the RNA/EtOH mixtures were loaded into the columns. Finally, the columns were centrifuged at 16 000g for 30 s to remove the flow-through and bind RNA. Following these steps, the procedure was performed according to manufacturer's instructions and including DNase treatment (Qiagen Italia, Milano, Italy) on the purification columns. Four pools for each chromatin configuration (CC\_GV0, CC\_GV1, CC\_GV2 and CC\_GV3) were used for microarray analysis and an additional four pools for each chromatin configuration (from independent collections) were used for microarray validation by quantitative reverse-transcriptase-PCR (qRT-PCR). Total RNA purity, integrity and concentration were evaluated using a 2100-Bioanalyzer (Agilent Technologies, Palo Alto, CA, USA) with the RNA PicoLab Chip (Agilent Technologies). All extracted samples were of good quality with an RNA integrity number of >7.4.

### RNA amplification, sample labeling and microarray hybridization

To generate enough material for the hybridization, RNA samples were linearly amplified according to the EmbryoGene pipeline. Antisense RNA (aRNA) was produced using the RiboAmp HS RNA amplification kit (Applied Biosystems, Thermo Fisher Scientific). After two amplification rounds of 6 h each, the aRNA output was quantified using the NanoDrop ND-1000 (NanoDrop Technologies, Wilmington, DE, USA) (Gilbert et al., 2009, 2010). Then, for each sample, 4 µg of aRNA was labeled using the

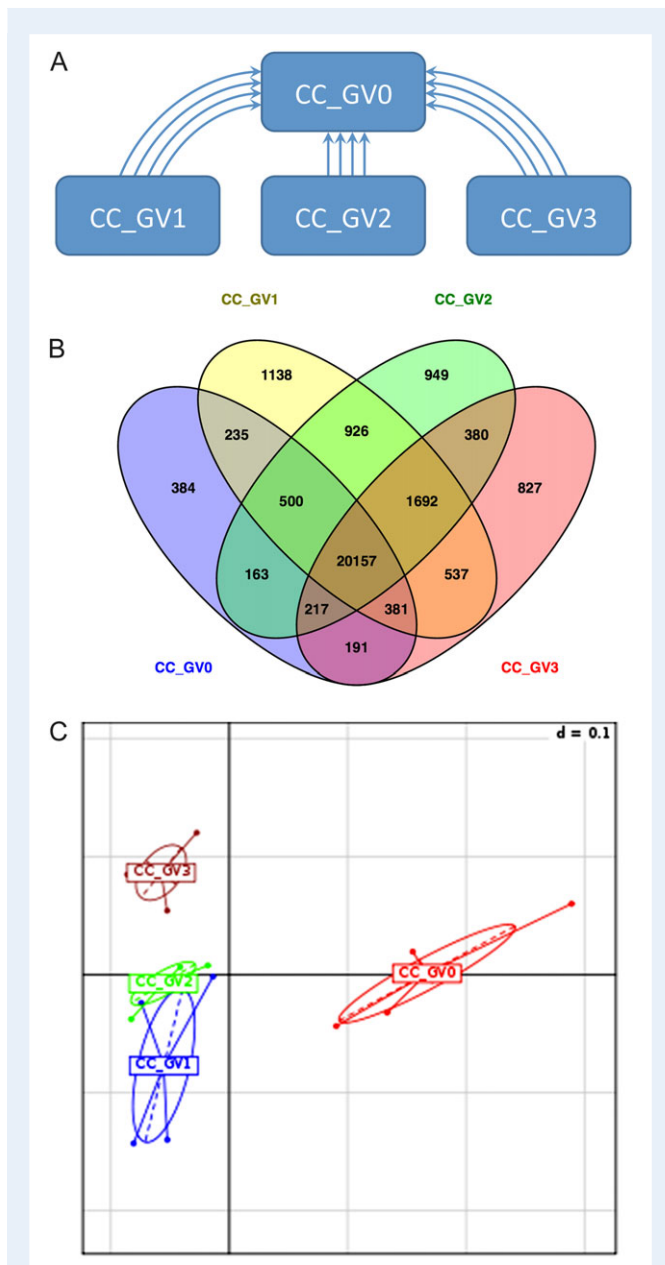


**Figure 1** Microarray analysis of CC isolated from oocytes with different large-scale chromatin configuration. **(A)** Experimental design. CC associated with oocytes with GV0, GV1, GV2 and GV3 chromatin configuration were isolated and subjected to microarray analysis. The hybridizations were performed using a reference design, where CC isolated from oocytes with GV1, GV2 and GV3 chromatin configuration were compared with CC isolated from GV0 oocytes (CC\_GV0 vs. CC\_GV1; CC\_GV0 vs. CC\_GV2; CC\_GV0 vs. CC\_GV3). In each contrast, the CC\_GV0 group represents the reference group. Overall, 12 hybridizations corresponding to the 4 biological replicates and 3 comparisons were performed. **(B)** Venn's diagram showing commonly expressed probes in the four experimental groups. Diagram was generated using the online tool VENNY 2.0 (Oliveros, J.C. (2007–2015) Venny. An interactive tool for comparing lists with Venn's diagrams. <http://bioinfogp.cnb.csic.es/tools/venny/index.html>), in which the lists of expressed probes in each group were uploaded. **(C)** BGA of the CC microarray data, in which the samples

ULS Fluorescent Labeling Kit for Agilent arrays (with Cy3 and Cy5) (Kreatech Diagnostics, Amsterdam, The Netherlands). The labeled product was then purified with the Pico-Pure RNA Isolation Kit. Labeling efficiency was measured using the Nano-Drop ND-1000. Samples from the four biological replicates, representing six different weeks of CC collection, were hybridized on a custom bovine embryo-specific Agilent 44 K microarray slide (Robert *et al.*, 2011). The hybridizations were performed using a reference design, where CC isolated from oocytes bearing the GV1, GV2 or GV3 chromatin configuration were compared with CC isolated from GV0 oocytes (CC\_GV0 vs. CC\_GV1; CC\_GV0 vs. CC\_GV2; CC\_GV0 vs. CC\_GV3). Thus, the reference group in the contrast is always represented by the CC\_GV0 group. Overall, 12 hybridizations corresponding to the 4 biological replicates and 3 comparisons were performed (Fig. 1A). A total of 825 ng of each labeled sample (Cy3 and Cy5) was incubated in a solution containing 10 $\times$  blocking agent and 25 $\times$  fragmentation buffer in a volume of 55  $\mu$ l at 60 $^{\circ}$ C for 15 min and were put on ice immediately after. Then, 55  $\mu$ l of 2 $\times$  GEx Hybridization Buffer HI-RPM was added for a total volume of 110  $\mu$ l. The hybridization mix (100  $\mu$ l) was added onto the array and hybridization was performed at 60 $^{\circ}$ C for 17 h using an Agilent Hybridization chamber in a rotating oven. After washing and drying steps, the slides were scanned using the Tecan PowerScanner microarray scanner (Tecan Group Ltd, Männedorf, Switzerland) and features were extracted using ArrayPro 6.4 Analyzer (Media Cybernetics, Bethesda, MD, USA).

### Microarray data analysis

Microarray data analysis was performed according to the EmbryoGENE pipeline. Intensities files were uploaded to ELMA software (EmbryoGENE LIMS Microarray Analysis, <http://elma.embryogene.ca/>), to run the quality control module.

To detect the presence or absence of the signal for each spot present on the slide, microarray data sets generated by ELMA were analyzed and an arbitrary cut-off corresponding to the mean intensity of the background level plus twice the standard deviation (SD) of the background was used. A Venn diagram was created using the online tool VENNY to show present and common probes between groups. Moreover, a between-group analysis (BGA) was performed to classify the samples according to their transcriptomic profiles (Culhane *et al.*, 2002).

To calculate the gene expression fold change for each contrast individually (CC\_GV0 vs. CC\_GV1; CC\_GV0 vs. CC\_GV2; CC\_GV0 vs. CC\_GV3) microarray data sets generated by ELMA were analyzed with the FlexArray microarray analysis software, Version 1.6.1 (Blazejczyk *et al.*, 2007). Briefly, raw data were subjected to a simple background subtraction, normalized within each array (Loess) and a Limma simple analysis was performed to obtain the fold change values. The reference group in the contrasts is represented by the CC\_GV0 group.

In addition, data sets generated by ELMA were subjected to microarray analysis of variance (MAANOVA) that was conducted considering the four experimental groups and by using the CC\_GV0 as a reference group. Differences were considered as statistically significant with a *P*-value of

are classified according to their transcriptomic profile (Culhane *et al.*, 2002) using the online tool available within the EmbryoGENE LIMS and Microarray Analysis (ELMA) pipeline. The plot illustrates the global distribution of transcriptome data (expressed probes) from the four experimental groups (CC from GV0, GV1, GV2 or GV3 oocytes) and the four biological replicates (dots in each group). The relative distance between each group indicates the global transcriptional differences among CC isolated from oocytes with different chromatin configurations.

<0.05. After MANOVA analysis, probes were grouped in clusters according to their expression profile using the mFuzz Bioconductor package (Kumar and Futschik, 2007).

Finally, the gene lists generated by our analysis were examined using Ingenuity Pathway Analysis (Ingenuity Systems, Mountain View, CA, USA). All statistically significant genes ( $P$ -value < 0.05) were uploaded to the application. The functional analysis identified the biological functions that were most significant to the molecules in the database.

## cDNA preparation and qRT-PCR

The validation of microarray results was performed by qRT-PCR using four independent biological replicates (each pool containing CC derived from 10 COC). For each sample, 1 ng of total RNA was reverse transcribed using the SuperScript First-Strand Synthesis for RT-PCR (Invitrogen—Thermo Fisher Scientific) with oligo-dT primers following the manufacturer's recommendations. Primer sequences used for real-time RT-PCR are provided in Supplementary Table 1. Primers were designed using the Primer3 online tool (<http://primer3.ut.ee/>) from sequences obtained using the UMD3.1 assembly of the bovine genome. Specificity of each primers pair was confirmed by electrophoresis analysis on a standard 2% agarose gel and sequencing analysis.

The PCR products were purified with the QIAquick PCR Purification kit (Qiagen), quantified using the Qbit 2.0 fluorometer and Qubit dsDNA HS Assay Kit (Invitrogen—Thermo Fisher Scientific). Serial dilutions of the PCR products (ranging from  $2 \times 10^{-4}$  to  $2 \times 10^{-8}$  ng/ $\mu$ l) were then used to create the standard curves for the evaluation of the amplification efficiencies. Quantitative real-time PCR was performed on an iQ5 (Bio-Rad, Laboratories S.r.l., Segrate, Italy) using SYBR incorporation. Each qPCR, in a final volume of 20  $\mu$ l, contained the cDNA corresponding to 1 ng of RNA extracted, 0.1  $\mu$ M of each primer and 1 $\times$  SYBR mix (iQ Universal SYBR Green Supermix, Bio-Rad). The PCR conditions used for all genes were as follows: a denaturing step of 30 s at 95°C, followed by 40 PCR cycles (95°C for 30 s; 57°C for 1 min), a melting curve (55°C for 1 min and a step cycle starting at 55°C, up to 94.5°C). PCR specificity was confirmed by melting-curve analysis.

For each gene tested, four independent biological replicates were used. Analysis of gene expression stability over the four groups was performed using the GeNorm algorithm (Vandesompele et al., 2002) through Biogazelle's qBase+ software (Biogazelle, Zwijnaarde, Belgium). Beta actin (ACTB), glyceraldehyde-3-phosphate dehydrogenase (GAPDH) and hypoxanthine phosphoribosyl transferase I (HPRT1) were identified as the most stable genes among the different groups, with  $M$ -value <1.5, and thus used as reference genes. Complementary DNA quantification was performed with the iQ5 Optical System Software Version 2.0 (Bio-Rad) using the delta-delta Ct method, where CC from GV0 were used as a reference group.

## Active caspase-positive cells analysis

Dispersed CC preparations (Luciano et al., 2000) isolated from single oocytes with different chromatin configurations (CC\_GV0, CC\_GV1, CC\_GV2 and CC\_GV3) were collected as described above and processed through the CaspaTag™ Pan-Caspase *In-Situ* Assay Kit (Merck Millipore, Billerica, MA, USA), a methodology based on Fluorochrome Inhibitors of Caspases (FLICA) to detect active caspase in cells undergoing apoptosis, following the manufacturer's specification sheet with slight modifications. Briefly, dispersed CC were plated in four-well plate for 3 h in TCM199 supplemented with 0.68 mM L-glutamine, 25 mM NaHCO<sub>3</sub>, 0.2 mM sodium pyruvate and 0.4% fatty acid-free BSA at 38.5°C and 5% CO<sub>2</sub>, to allow them to adhere to the plate. Subsequently, cells were cultured for one additional hour in the presence of a carboxyfluorescein-labeled inhibitor of caspases. After washings and fixation in 10% formaldehyde, cells

were detached by gently pipetting and moved on a glass slide. When dried, cells were covered with the antifade medium Vecta Shield (Vector Laboratories, Burlingame, CA, USA) supplemented with 1  $\mu$ g/ml 40,6-diamidino-2-phenylindole (DAPI) and analyzed under fluorescent microscopy (Nikon Eclipse E600). For each sample, 10/15 fields were randomly chosen and results were expressed as the number of active caspase-positive cells over the total number of cells observed.

## Assessment of the relationship between COC features and oocyte chromatin configuration

In order to establish morphological criteria that would allow for the collection and/or selection of a population of COC enriched in one of the three GV chromatin configurations (GV1, GV2 or GV3), the relationship between the oocyte chromatin configuration and either (i) the size of the follicle from which the COC was isolated or (ii) the morphology of the corresponding COC was assessed.

With this aim, in a first set of experiments, follicle sizes were determined with a ruler by measuring their visible diameter on the surface of the ovary. COC were collected from 2 to 4 mm, 4–6 or >6 mm antral follicles. In the second set of experiments, COC were collected from 2 to 8 mm antral follicles. In any case, only COC suitable for standard IVP procedure were included in the study. After the first selection, COC were further divided into three groups on the basis of morphological characteristics previously described (Blondin and Sirard, 1995; Hazeleger et al., 1995): Class 1, with homogeneous ooplasm and compact CC; Class 2, with minor granulation of the ooplasm with compact CC; Class 3, with highly granulated ooplasm and slight expansion of CC layers (Fig. 6B) (Gordon, 2003; Stringfellow and Givens, 2010).

In both cases, COC were finally denuded, fixed in a methanol and Dulbecco's Phosphate-Buffered Saline (DPBS) solution (60:40), and stained with DAPI for the assessment of chromatin configuration under fluorescence microscopy as above described.

## Glucose-6-phosphate dehydrogenase activity determination by brilliant cresyl blue staining

COC isolated from 2 to 8 mm antral follicles and selected as above described were separated into two groups based on the morphological criteria as Class 1 and Class 2/3 (Fig. 6B). COC were then stained with brilliant cresyl blue (BCB) as previously described (Torner et al., 2008), with slight modifications. Briefly, COC were incubated in 26  $\mu$ M BCB diluted in DPBS with calcium and magnesium, and supplemented with 0.4% of BSA for 90 min at 38.5°C in humidified air atmosphere. After washing, CC were removed and oocytes were examined under a stereomicroscope. Oocytes were classified as BCB negative (BCB-), when the oocyte showed a colorless cytoplasm, or BCB positive (BCB+) where oocytes showed different grades of blue/violet color.

## *In-vitro* pre-maturation, IVM, IVF and embryo culture

For IVP experiments, only COC from 2 to 8 mm middle antral follicles collected as above described were used. After isolation and selection, COC were divided based on the morphological criteria as Class 1, Class 2 and Class 3 as above described. Groups of 20–30 COC belonging to Class 1, Class 2/3 or unsorted COC (a mix of Class 1, Class 2 and Class 3, corresponding to the population of COC that is commonly used in standard IVP procedures) were subjected to standard IVP (IVM, IVF and *in-vitro* embryo culture (IVC)) with or without a *In-vitro* pre-maturation (pre-IVM) culture step (Franciosi et al., 2014). To avoid meiotic resumption before pre-IVM,

COC were classified in HMI 199 supplemented with the non-selective PDE inhibitor 3-isobutyl-1-methyl-xanthine (IBMX) at the final concentration of 0.5 mM (Lodde *et al.*, 2013). Pre-IVM consisted of culture for 6 h in M199 added with 0.68 mM L-glutamine, 25 mM NaHCO<sub>3</sub>, 0.4% BSA fatty acid free, 0.2 mM sodium pyruvate, 10<sup>-4</sup> IU/ml of r-hFSH (Gonal-F, Serono, Rome, Italy) and 10 μM cilostamide in humidified air under 5% CO<sub>2</sub> at 38.5°C (Franciosi *et al.*, 2014).

For IVM, COC (immediately after collection or after 6 h of pre-IVM) were cultured for 22 h in M199 added with 0.68 mM L-glutamine, 25 mM NaHCO<sub>3</sub>, 0.4% BSA fatty acid free, 0.2 mM sodium pyruvate and 0.1 IU/ml of r-hFSH (Gonal-F, Merck Serono, Darmstadt, Germany) at 38.5°C in 5% CO<sub>2</sub> as described by Luciano *et al.* (2005).

IVF and IVC were carried out as previously described (Luciano *et al.*, 2005). At the end of culture period (*d* + 8), the blastocyst rate was assessed under a stereomicroscope. The embryos were then fixed in 60% methanol in DPBS and the cell nuclei were counted under a fluorescence microscope after staining with 0.5 mg/ml of propidium iodide (Luciano *et al.*, 2005).

**Table 1** Number of differentially expressed probes (*P* < 0.05).

	Total	Fold change >2 <sup>a</sup>	Fold change >-2 <sup>a</sup>
CC_GV0 vs. CC_GV1	112	77	35
CC_GV0 vs. CC_GV2	127	42	85
CC_GV0 vs. CC_GV3	204	82	122

<sup>a</sup>Note: that CC\_GV0 represents the reference group; therefore, positive fold change means upregulation in GV1, GV2 or GV3 when compared with CC\_GV0, while negative fold change means downregulation in GV1, GV2 or GV3 when compared with CC\_GV0.

## Statistical analysis

Experiments were repeated at least three times. Data were analyzed by one-way ANOVA followed by Newman-Keuls Multiple Comparison test using Graph Pad Prism version 6.0 h. Data are presented as mean ± SEM. *P* values < 0.05 were considered as statistically significant. For each experiment, the specific test used is indicated in the figure legend.

## Results

### Microarray results

To gain insights into transcriptomic profiles of CC associated with oocytes with different large-scale chromatin configurations, three microarray comparisons using the EmbryoGENE bovine microarray were performed. This microarray includes 42 242 probes, of which 31 138 represent reference genes, novel untranscribed regions, 3'-untranslated region variants and alternatively spliced exons (Robert *et al.*, 2011).

As shown in Fig. 1A, the hybridizations were performed using a reference design, where the CC isolated GV1, GV2 or GV3 chromatin configuration were compared with CC from GV0 oocytes (CC\_GV0 vs. CC\_GV1; CC\_GV0 vs. CC\_GV2; CC\_GV0 vs. CC\_GV3; the reference group in the contrast is represented by the CC\_GV0 group). Microarray data were deposited in the National Center for Biotechnology Information (NCBI)'s Gene Expression Omnibus (Edgar *et al.*, 2002), and are accessible through GEO series accession number GSE79886 (<http://www.ncbi.nlm.nih.gov/geo/query/acc.cgi?acc=GSE79886>).

Considering the threshold used to detect the presence/absence of the spots on the microarray slides, a total of 20 155 probes were commonly expressed in all the four groups (Fig. 1B), while 384, 1 138, 949 and 827 were expressed only in CC\_GV0, CC\_GV1, CC\_GV2 and CC\_GV3, respectively. As shown in Fig. 1C, the BGA revealed the

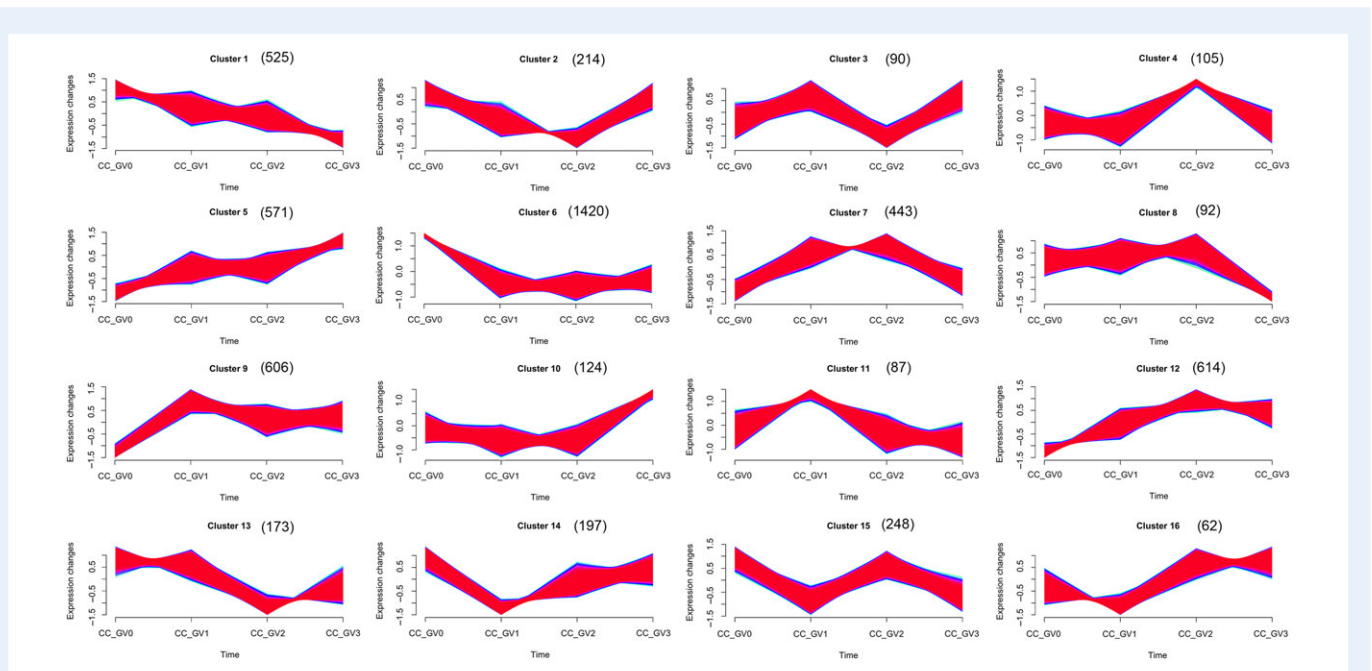


**Figure 2** Clusters analysis. Graphs represent the 16 clusters generated by the mFuzz clustering analysis (Kumar and Futschik, 2007). For each cluster, the number of statistically significant probes that best fit to each profile is indicated between brackets. Note: cluster #6 is the one with the higher number of best fit probes.

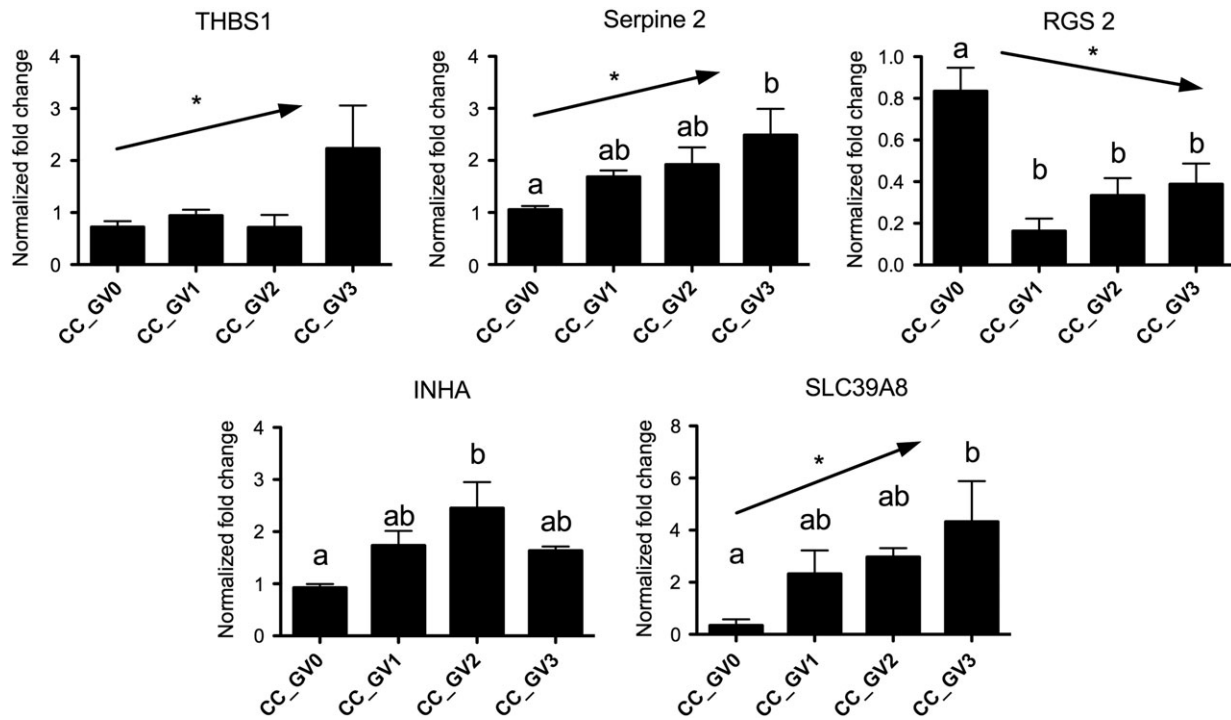


**Figure 3** qRT-PCR validation of the microarray results. Validation of microarray data by means of qRT-PCR. Graphs indicate relative expression levels of selected genes in CC isolated from oocytes with GV0, GV1, GV2 or GV3 chromatin configuration; expression levels for each gene were normalized using ACTB, GAPDH and HPRT1 as reference genes. Relative fold changes were calculated using the delta-delta Ct method using CC\_GV0 as a reference group. Data were analyzed by one-way ANOVA followed by Newman-Keuls multiple comparison test and are expressed as means  $\pm$  SEM. Different superscripts indicate significant differences between groups ( $P < 0.05$ ). Where applicable, test for linear trend was also conducted (\*,  $P < 0.05$ ). Note: the selected genes, with accession number, primer sequences, annealing temperature and product size are as in Supplementary Table I.

global transcriptional differences among CC isolated from oocytes with different chromatin configurations. Considering the biological replicates (dots) within each group, the CC\_GV0 and CC\_GV1 groups displayed more variation (increased distance between the dots) compared with GV2 and GV3. Moreover, CC\_GV0 and CC\_GV3 groups were characterized by unique gene expression profiles, while some minimal overlapping existed between CC\_GV1 and CC\_GV2 groups.

The MAANOVA algorithm revealed that 5571 probes were significantly differentially expressed ( $P < 0.05$ ) between groups, of which 112, 127 and 204 presented a fold change difference more than  $\pm 2$  in CC\_GV0 vs. CC\_GV1, CC\_GV0 vs. CC\_GV2 and CC\_GV0 vs. CC\_GV3, respectively (Table I). Clustering analysis with the mFuzz Bioconductor package generated 16 clusters representing the main profiles of transcription modulation (Fig. 2). Of the 5571 significantly differentially expressed probes, 25.49% best fitted with cluster #6 profile (downregulation between CC\_GV0 and CC\_GV1 and relatively stable low levels in successive groups). Clusters #1 (constant decrease from CC\_GV0 to CC\_GV3), cluster #5 (constant increase from CC\_GV0 to CC\_GV3), cluster #9 (upregulation between CC\_GV0 and CC\_GV1 and relatively stable levels in successive groups) and cluster #12 (upregulation from CC\_GV0 to CC\_GV2 and relatively stable levels from CC\_GV2 to CC\_GV3) each included  $\sim 10\%$  of the total probes, while the other clusters included low numbers of probes (Fig. 2).

A subset of five genes was selected, according to their significant changes in the three comparisons after FlexArray analysis and their known biological functions, to validate the microarray results by qRT-PCR. The chosen genes were Thrombospondine 1 (THBS1), Serpine 2, regulator of G-protein signaling 2 (RGS2), inhibin alpha (INHA) and solute carrier family 39, member 8 (SLC39A8, Supplementary Table I). Overall, qRT-PCR results were consistent with the microarray data (Fig. 3).

### IPA-based functional analysis

Lists of genes that best fitted each of the main clusters (#1, #5, #6, #9 and #12) were submitted to IPA in order to identify the most relevant molecular and cellular functions associated with each cluster (Table II). The genes included in cluster #1 were related to biological processes such as 'cell cycle' and 'cell death and survival', whereas genes included in cluster #5 were more related to molecular processes such as 'gene expression', 'RNA post transcriptional modification' and 'protein synthesis'. Interestingly, 'lipid metabolism' and 'small molecule biochemistry' were the most significant functions identified in clusters #6, #9 and #12.

Moreover, in order to gain insights into the molecular and cellular pathways that were likely affected in CC during oocyte chromatin compaction, gene lists obtained from each contrast individually by

**Table II Molecular and cellular functions of best fit genes in most represented clusters identified by IPA ( $P < 0.05$ ).**

Molecular and cellular functions	P-value	#Molecules
<i>Cluster 1</i> (↘↘↘) (constant decrease from CC_GV0 to CC_GV3)		
Cell cycle	1.73E-02–3.49E-09	74
Cellular assembly and organization	1.73E-02–3.49E-09	48
DNA replication, recombination and repair	1.73E-02–3.49E-09	67
Cellular movement	1.73E-02–5.10E-06	30
Cell death and survival	1.73E-02–6.41E-06	99
<i>Cluster 5</i> (↗↗↗) (constant increase from CC_GV0 to CC_GV3)		
RNA post-transcriptional modification	1.24E-02–2.06E-05	17
Protein synthesis	8.88E-03–3.87E-05	43
Gene expression	1.88E-02–5.04E-05	72
Cell signaling	1.88E-02–3.43E-04	15
Vitamin and mineral metabolism	1.88E-02–3.43E-04	8
<i>Cluster 6</i> (↘→→) (downregulation between CC_GV0 and CC_GV1 and relatively stable low levels in successive groups)		
Lipid metabolism	2.16E-02–8.40E-05	103
Small molecule biochemistry	2.23E-02–8.40E-05	141
Cellular assembly and organization	2.13E-02–2.01E-04	60
Cellular development	2.31E-02–2.23E-04	176
Cellular growth and proliferation	2.31E-02–2.23E-04	260
<i>Cluster 9</i> (↗→→) (upregulation between CC_GV0 and CC_GV1 and relatively stable levels in successive groups)		
Lipid metabolism	1.97E-02–2.65E-05	32
Small molecule biochemistry	1.97E-02–2.65E-05	46
Molecular transport	1.97E-02–2.81E-05	69
Cellular assembly and organization	1.97E-02–1.22E-04	31
Cellular function and maintenance	1.97E-02–1.22E-04	37
<i>Cluster 12</i> (↗↗→) (upregulation from CC_GV0 to CC_GV2 and relatively stable levels from CC_GV2 to CC_GV3)		
Lipid metabolism	2.18E-02–8.79E-05	49
Small molecule biochemistry	2.18E-02–8.79E-05	71
Vitamin and mineral metabolism	2.15E-02–8.79E-05	23
Cell-to-cell signaling and interaction	2.15E-02–8.79E-05	59
Cellular movement	1.86E-02–9.96E-05	43

FlexArray (CC\_GV0 vs. CC\_GV1; CC\_GV0 vs. CC\_GV2; CC\_GV0 vs. CC\_GV3) were uploaded to IPA and analyzed considering the fold change difference for each gene. Interestingly, one of the main affected functions in each contrast was 'cell death and survival' (Table III). Moreover, as shown in Fig. 4, the number of apoptosis-related genes that were deregulated increased substantially from CC\_GV0 vs. CC\_GV1 to CC\_GV0 vs. CC\_GV3 contrasts. Importantly, IPA revealed that apoptosis is predicted to be inhibited in CC\_GV1 and CC\_GV2, while it is activated in CC\_GV3 (Fig. 4, gene lists shown in Fig. 4 are provided as Supplementary Table 2).

### Active caspase-positive cells analysis

In order to validate the *in-silico* functional prediction (generated by IPA) that CC\_GV3 is more prone to apoptosis, we analyzed the susceptibility of CC isolated from oocytes with different chromatin configurations to undergo apoptosis.

It has been shown that apoptotic cell death of granulosa cells is the molecular mechanism underlying follicle atresia (Jolly *et al.*, 1994).

A previous study demonstrated that the dissociation of both mural granulosa cells and CC triggers apoptosis in both cell subsets (Luciano *et al.*, 2000). Therefore, we used CC dissociation as a 'stress test' in order to assess whether chromatin compaction (from GV0 to GV3) was associated with an increased tendency of the oocyte's associated CC to undergo apoptosis. CC isolated from single oocytes with different chromatin configurations (CC\_GV0, CC\_GV1, CC\_GV2 and CC\_GV3) were isolated and *in-vitro* cultured for 3 h and then assayed for pan-caspase activity. As shown in Fig. 5, the percentage of caspase-positive cells was significantly lower in CC from GV0 oocytes, whereas it increased in CC from GV1 and GV2 oocytes, reaching the highest value in CC from GV3 oocytes, as predicted by IPA.

### Relationship between COC features and oocyte chromatin configuration

The findings that CC isolated from oocytes with different chromatin configurations differ in their transcriptomic profiles and in their



**Table III Molecular and cellular functions identified by IPA ( $P < 0.05$ , fold change higher than  $\pm 2$ ) in each contrast (CC\_GV0 vs. CC\_GV1, CC\_GV0 vs. CC\_GV2, CC\_GV0 vs. CC\_GV3, where CC\_GV0 represents the reference group).**

Molecular and cellular functions	P-value	#Molecules
CC_GV0 vs. CC_GV1		
Cell death and survival	4.23E-03–2.69E-08	60
Cellular function and maintenance	4.28E-03–3.48E-07	64
Cellular movement	4.31E-03–5.75E-07	42
Cellular growth and proliferation	3.51E-03–7.05E-07	63
Cell-to-cell signaling and interaction	4.17E-03–9.85E-07	49
CC_GV0 vs. CC_GV2		
Cell death and survival	7.77E-03–2.51E-08	73
Cellular function and maintenance	8.19E-03–4.69E-08	60
Cellular growth and proliferation	7.51E-03–5.65E-07	76
Cellular movement	7.72E-03–9.42E-07	49
Cell morphology	8.19E-03–1.12E-05	53
CC_GV0 vs. CC_GV3		
Cell death and survival	1.78E-03–1.22E-15	107
Cellular development	1.95E-03–7.66E-11	109
Cell cycle	1.78E-03–1.10E-10	61
Cellular growth and proliferation	1.95E-03–1.25E-10	114
Cell morphology	1.70E-03–1.16E-08	67

susceptibility to undergo apoptosis, lead us to hypothesis that COC isolated from middle antral follicles bearing oocytes with different chromatin configurations (GV1, GV2 or GV3) could respond differently to specific *in-vitro* cultural conditions.

To test this hypothesis, and considering that it is technically not possible to directly identify the chromatin configuration without DNA staining after CC removal, we first looked for possible morphological markers that could be related to the chromatin configuration of the corresponding oocyte, and that therefore could be used to isolate a population of COC from middle antral follicle enriched in one of the GV stages (GV1, GV2 or GV3). Precisely, we considered the possible relationship between chromatin configuration and (i) the size of the follicle and (ii) the morphology of the COC, using morphological criteria commonly accepted by the scientific community and clearly recognizable under a stereomicroscope. These studies revealed a relationship between the oocyte chromatin configuration and the morphology of the COC but not with the size of the follicle from which they originate (Fig. 6). In fact, oocytes with GV1, GV2 and GV3 chromatin configuration were equally distributed in follicle of 2–4, 4–6 and > 6 mm in diameter (Fig. 6A). On the other hand, as shown in Fig. 6B, when isolated and additionally sub-grouped into three classes based on their morphology (Blondin and Sirard, 1995), Class I COC (with homogeneous ooplasm and compact CC) was the only one in which oocytes with GV1 chromatin configuration could be found,

while oocytes with GV1 chromatin configuration were almost absent in Class 2 and 3 COC (minor granulation of the ooplasm with compact CC, or highly granulated ooplasm and/or few outer layers CC showing expansion in Classes 2 and 3, respectively),

Furthermore, BCB staining of Classes 1, 2 and 3 COC indicated that Class 1 COC are in an earlier stage of differentiation when compared with Class 2 and 3 COC, giving additional (indirect) confirmation that chromatin compaction is associated with oocyte (and accompanying CC) differentiation. Indeed as shown in Fig. 6C, the percentage of BCB-negative oocytes was significantly higher in Class 1 than in Class 2/3 COC ( $P < 0.05$ ).

## Effect of pre-IVM treatment on oocyte developmental competence

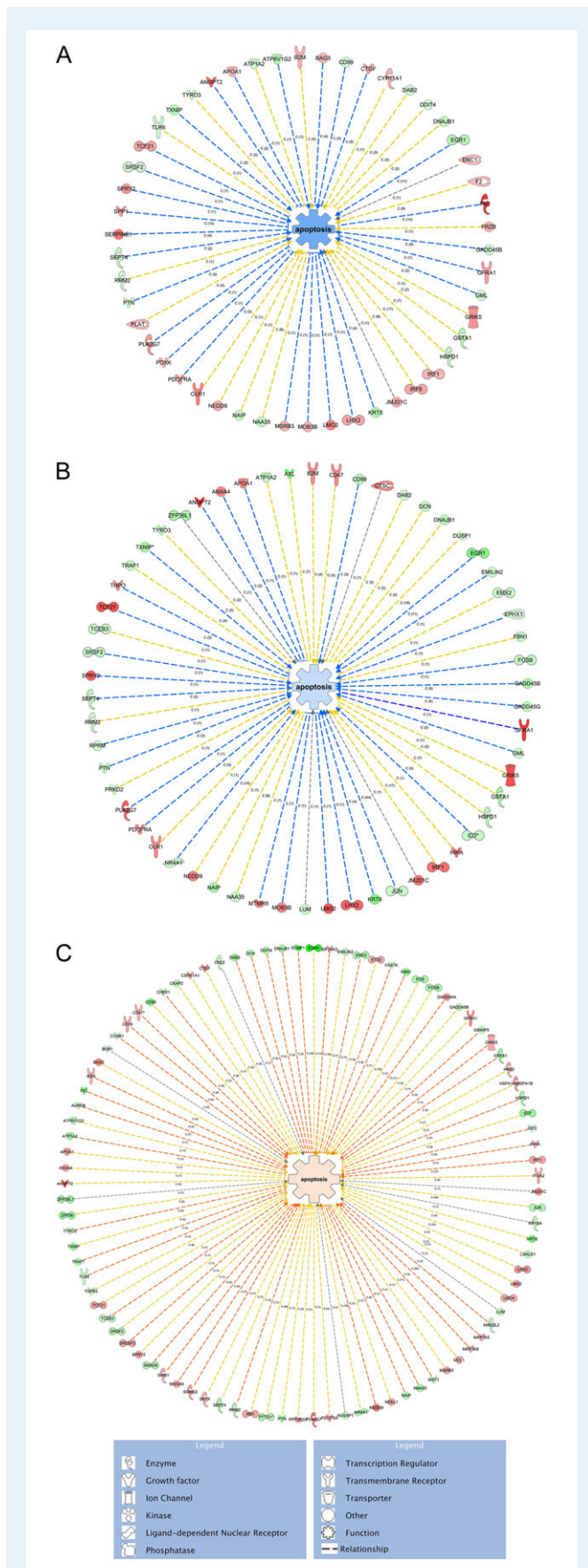
Having established that Class 1 and Class 2/3 COC differ in the relative percentage of oocytes with different chromatin configuration, and that Class 1 was the only class enriched with GV1 oocytes, we tested the hypothesis that these classes respond differently to specific *in-vitro* cultural conditions.

As shown in Fig. 7, when subjected to standard IVP procedures (within a regular IVM protocol), Class 1 COC showed a limited embryonic developmental competence (Fig. 7). Indeed after 7 days of culture both the blastocyst rate and mean blastocyst cell number per embryo were significantly lower in Class 1 COC when compared with the Class 2/3 groups ( $P < 0.05$ ). As expected, the group composed of the mix of Class 1, 2 and 3 COC, which correspond to the unsorted group of COC commonly used in IVP protocols, showed intermediate values between Class 1 and Class 2/3 COC. On the other hand, pre-IVM treatment increased significantly the developmental capability (blastocyst rate and mean blastocyst cell number per embryo) of Class 1 COC and had no effect on the mixed group, while it reduced the developmental competence of Class 2/3 COC.

## Discussion

The present work provides the first comprehensive transcriptome analysis of bovine CC associated with oocytes with a specific large-scale chromatin configuration. This is particularly relevant as chromatin configuration is indicative of the state of oocyte differentiation in the antral follicle before dominance emergence in naturally cycling animals (Lodde et al., 2007, 2008, 2009). Transcriptomic data analysis confirmed the hypothesis that features of the cumulus oophorus investment change along with oocyte chromatin compaction. Interestingly, results of the BGA analysis, that gives information on the overall transcriptomic profile of each biological sample, are in accordance with the global change in distribution of transcriptomic data obtained from oocytes with different chromatin configurations (compare Fig. 1C of the present study and Fig. 2 in Labrecque et al., 2015). Collectively, these data, and in particular the relative distance between each group, effectively confirm that global transcriptional differences exist among oocytes with different chromatin configurations as well as in their surrounding CC. Thus, the transcriptome of the whole COC changes along with the increase in chromatin compaction.

According to our previous morphological and functional studies, the present clustering analysis of microarray data revealed that major changes in terms of CC transcript differences occur during the



GV0-to-GV1 transition (Fig. 2). Indeed, the cluster profiles #6 and 9 (downregulation or upregulation between CC\_GV0 and CC\_GV1 and relatively stable low levels in successive groups) collect ~36% of the differentially expressed probes. Interestingly, *in-silico* functional analysis through IPA of the subsets of genes that best fitted with these two profiles revealed a major change of CC transcripts involved in lipid metabolism during the GV0-to-GV1 transition. Recent works showed that the lipid content in CC reflects the quality of the female gamete (Montani *et al.*, 2012; Auclair *et al.*, 2013) both in human (Matorras *et al.*, 1998) and in bovine (Kim *et al.*, 2001). It has been also recently reported that CC are able to protect the oocyte by storing elevated levels of free fatty acids from follicular fluid (Aardema *et al.*, 2013). In addition, studies in mice revealed that oocytes are deficient in cholesterol production and require CC to provide products of the cholesterol biosynthesis pathway, and suggest that oocytes promote cholesterol biosynthesis in CC through oocyte-derived paracrine factors, probably to compensate for their deficiency (Su *et al.*, 2008). Altogether, these data sustain the general idea that defective lipid metabolism inside the COC may be in part responsible for the lower meiotic and developmental competence of the oocyte. In this view, we can speculate that CC acquire the 'competence' of metabolizing lipids during the GV0–GV1 transition, which occurs during the early-to-middle stage of follicle development, and that the inability of GV0 oocytes to mature and develop into an embryo might be, at least in part, from an inappropriate capacity of the surrounding CC to metabolize lipids. Nevertheless, this hypothesis remains to be confirmed experimentally.

Gene expression profiles in CC have attracted great interest in the last years. In fact, a small biopsy of the cumulus oophorus could be easily collected before IVM, without perturbing oocyte viability, and assayed for expression of genes used as markers to predict the corresponding oocyte's quality. With this view, the present study confirms several previously reported markers associated with poor or high embryonic developmental potential in cattle, such as GATM or MANIAI (Bunel *et al.*, 2014, 2015). Notably, a similar approach has been conducted in the primed mouse model by comparing the transcriptomic profiles of CC isolated from antral oocytes with a non-surrounded nucleolus configuration (NSN, less compacted chromatin) and surrounded nucleolus configuration (SN, more compacted chromatin) (Zuccotti *et al.*, 1995; Vigone *et al.*, 2013). Compared to the present study in the cow, Vigone *et al.* found a relatively low number of differentially expressed genes with fold changes higher than 2. The difference of the animal model of course could explain this difference. Moreover, we cannot exclude that taking advantages of the gradual chromatin remodeling by considering two intermediate stages of compaction (GV1 and GV2) between the two extremes (GV0 and GV3) allowed the identification of a higher number of differentially expressed

**Figure 4** Functional analysis. IPA generated diagrams representing deregulated apoptosis-related genes ( $P < 0.05$ ; fold change higher than  $\pm 2$ ) in CC\_GV0 vs. CC\_GV1 (A), CC\_GV0 vs. CC\_GV2 (B) and CC\_GV0 vs. CC\_GV3. Note that apoptosis is predicted to be inhibited (blue) in CC\_GV1 and CC\_GV2, while it is activated (orange) in CC\_GV3. Gene lists are provided in Supplementary Table 2; genes in red are upregulated; genes in green are downregulated.

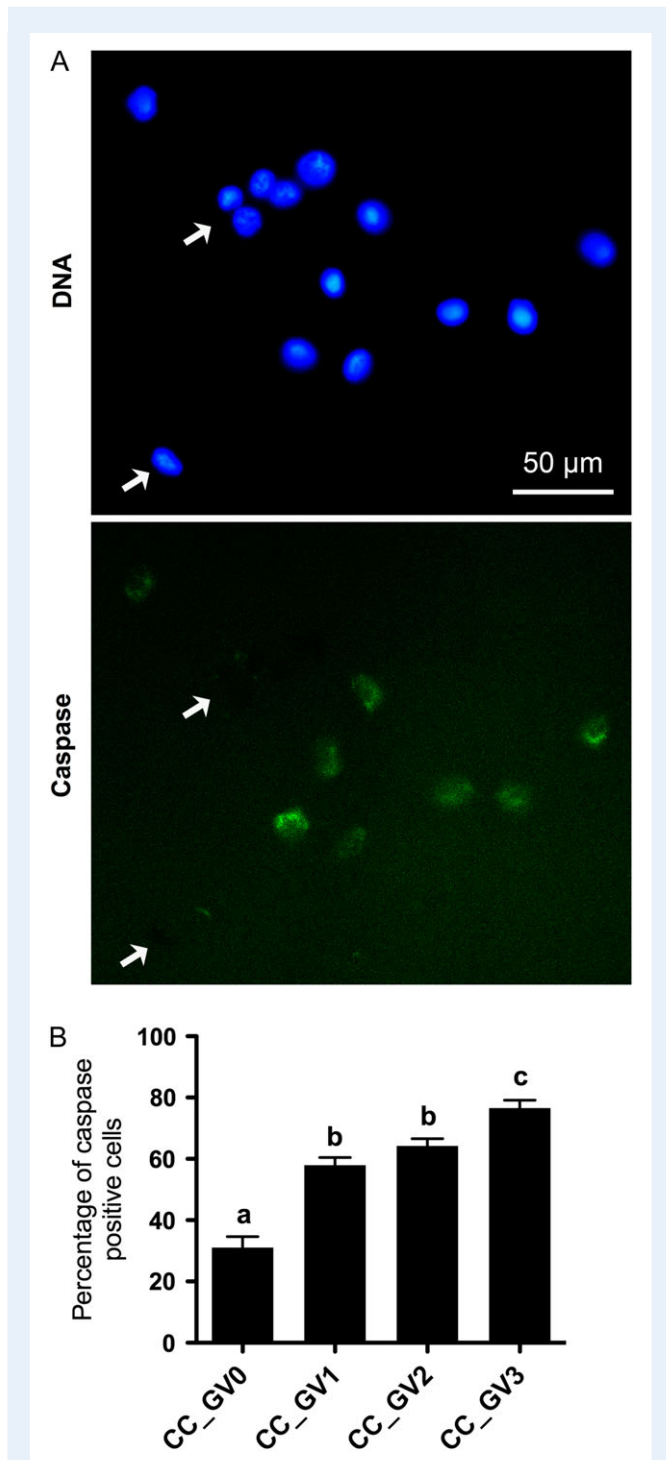


**Figure 5** Assessment of caspase activity in cells isolated from oocytes with different chromatin configurations. CC associated with oocytes with GV0, GV1, GV2 and GV3 chromatin configuration were isolated and assayed for Caspase activity after 3 h of culture using the CaspaTag™ Pan-Caspase In Situ Assay Kit. **(A)** Representative pictures show active caspase in cells undergoing apoptosis and negative (arrows) cells. **(B)** Graph shows the percentage of caspase-active cells in each GV category; data from three independent experiments were analyzed by one-way ANOVA followed by Newman-Keuls multiple comparison test; data are expressed as means  $\pm$  SEM; a,b,c: different superscripts indicate significant differences between groups ( $P < 0.05$ ).

genes. It may be possible indeed that mouse oocytes with intermediate configurations (Bouniol-Baly *et al.*, 1999; Bonnet-Garnier *et al.*, 2012), which are generally grouped together with one of the two extremes may limit the capacity for revealing certain differences. On the other hand, we found correspondence with some of the genes identified by Vigone *et al.*, such as Has2, which is upregulated in bovine CC\_GV3 and mouse SN oocytes when compared to GV0 and NSN oocytes, respectively. This sets the stage for further comparative studies between the mouse and the bovine models.

Importantly, besides the assessment and confirmation of genes with known function in the reproductive system, our analysis provides multiple new biomarkers that are potentially involved in oocyte competence acquisition. For example, our data indicate that SLC39A8 is one of the genes whose expression constantly increases in CC during the GV0-to-GV3 transition. SLC39A8, also known as ZIP8, encodes for a member of the SLC39 family of solute-carrier genes, which shows structural characteristics of zinc transporters (Wang *et al.*, 2012). Recently, it has been shown that the oocyte zinc content exerts important roles in oocyte function in mice, especially during meiotic maturation and fertilization (Kim *et al.*, 2010, 2011; Bernhardt *et al.*, 2011, 2012; Kong *et al.*, 2012; Tian and Diaz, 2012). Moreover, Lisle *et al.* suggested that CC regulate the amount of free Zinc in the oocyte during maturation (Lisle *et al.*, 2013). Interestingly, findings in mice show that acute dietary zinc deficiency during preconception (i.e. restricted to 3–5 days before ovulation) disrupts oocyte chromatin methylation and alters transcriptional regulation of repetitive elements, which is associated with severe defects of pre- and post-implantation embryonic development as well as of placental development (Tian and Diaz, 2013; Tian *et al.*, 2014). This is important since the period in which the mice were fed with a zinc deficiency diet in these studies corresponds to the final oocyte growth phase, when chromatin remodeling occurs (Albertini, 1992; Debey *et al.*, 1993; Zuccotti *et al.*, 1995; Bouniol-Baly *et al.*, 1999; De La Fuente *et al.*, 2004; Bonnet-Garnier *et al.*, 2012). These data clearly indicate that zinc plays important roles also before meiotic resumption and our data might set the stage for further investigation on the role of SLC39A8 as a possible player acting in the somatic compartment and involved in the control of oocyte zinc content, which is in turn important for the establishment of the oocyte epigenetic signature. Interestingly, in the mouse model, the zinc transporter SLC39A10 was found to be upregulated in CC from SN oocytes, when compared to NSN oocytes (Vigone *et al.*, 2013).

Importantly, besides the identification of single gene's function, the present data set gives the opportunity to find pathways and mechanisms that are set in place in the somatic compartment that ultimately affect oocyte quality. This has paramount implications in the development of oocyte culture systems specifically formulated to fulfill the specific needs of the oocyte at a specific stage and support their *in-vitro* development. For example, *in-silico* analysis of differentially expressed genes in the three contrasts through IPA, revealed that apoptosis is predicted to be inhibited in CC of GV1 and of GV2 (even if at a lower extent) while it is predicted to be activated in CC of oocytes with the highest degree of chromatin compaction (GV3). Among the apoptosis-related genes identified by IPA, angiopoietin 2 (ANGPT2) was the most upregulated gene in CC\_GV3 when compared to CC\_GV0. ANGPT2 is an antagonist of the angiogenic factor ANGPT1 that signals through the endothelial cell-specific Tie2 receptor tyrosine kinase. ANGPT2 disrupts the vascular remodeling ability of ANGPT1

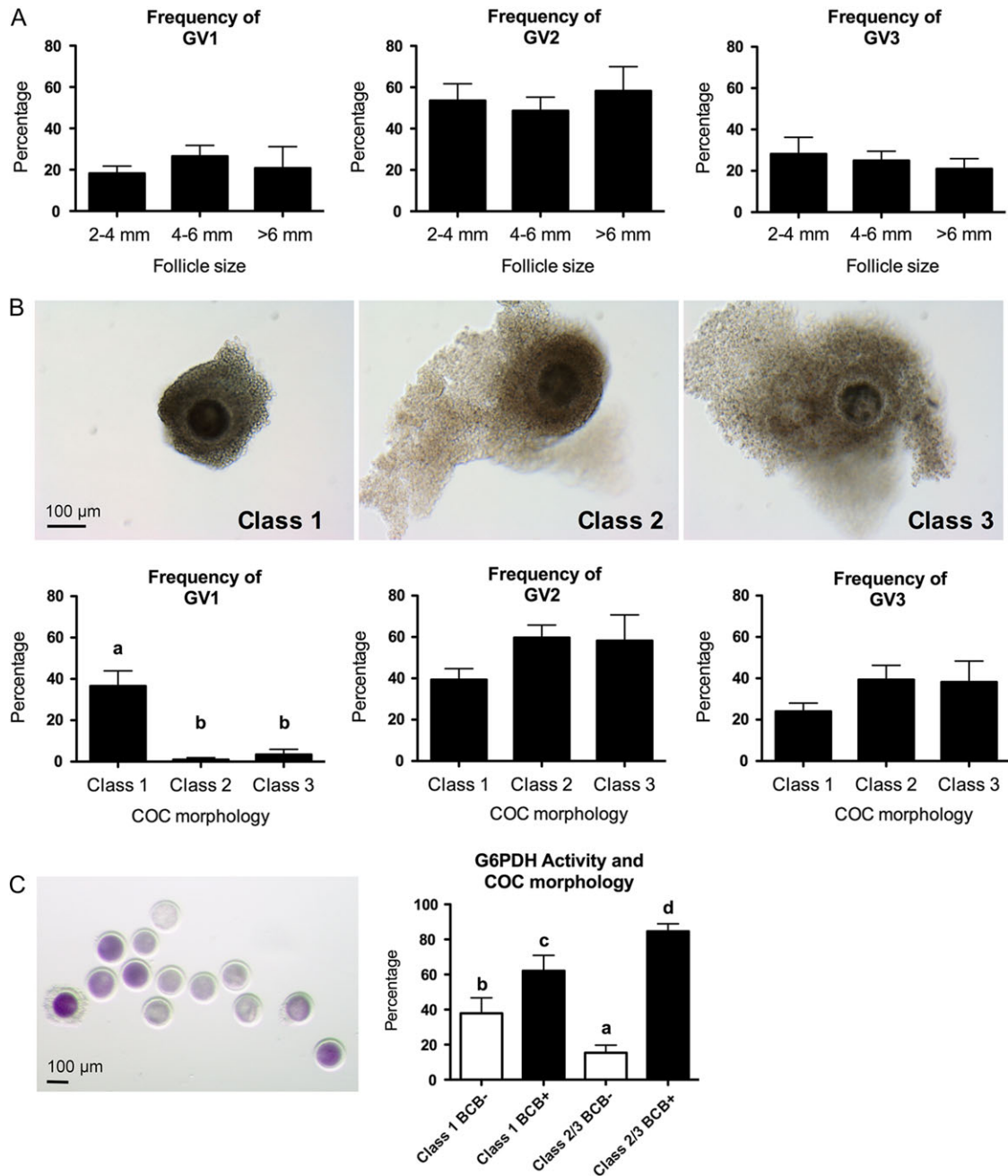


**Figure 6** Relationship between large-scale chromatin configuration, follicle size, COC morphology and oocyte glucose-6-phosphate dehydrogenase (G6PDH) activity. **(A)** COC were collected from follicles of different diameter and chromatin configurations were assessed after CC removal. Graphs show the frequency of GV1, GV2 and GV3 chromatin configurations in each follicle size category. A total of 277 oocytes (167, 52 and 52 from small, medium and large antral follicle, respectively) were used in this study in three independent experiments. Data were analyzed by one-way ANOVA. **(B)** After collection, COC were separated according to morphological criteria as shown in the representative pictures (*Class 1*: homogeneous ooplasm and absence of expansion of outer layer CC; *Class 2*: minor granulation of the ooplasm and/or beginning of expansion of outer layer CC; *Class 3*: highly granulated ooplasm and few CC layers showing expansion). After classification, CC were removed and the chromatin configuration was assessed. Graphs show the frequency of GV1, GV2 and GV3 chromatin configurations in each class. A total of 300 oocytes (101 Class 1, 119 Class 2 and 80 Class 3) were used in this study in three independent experiments. Data were analyzed by one-way ANOVA followed by Newman–Keuls multiple comparison test; a, b: different letters indicate significant differences,  $P < 0.05$ ). **(C)** After collection, COC were separated into Class 1 and Class 2/3 on the basis of their morphology and subjected to Brilliant Cresyl Blue staining (BCB). After removal of CC, oocytes were classified as BCB+ or BCB– as shown in the representative picture. Graph shows the percentage of BCB+ and BCB– oocytes in Class 1 and 2/3 COC. A total of 337 COC were analyzed (126 Class 1 and 211 of Class 2/3) in nine independent experiments. Data were analyzed by one-way ANOVA followed by Newman–Keuls multiple comparison test; data are expressed as means  $\pm$  SEM; a, b, c, d: different letters indicate significant differences ( $P < 0.05$ ).

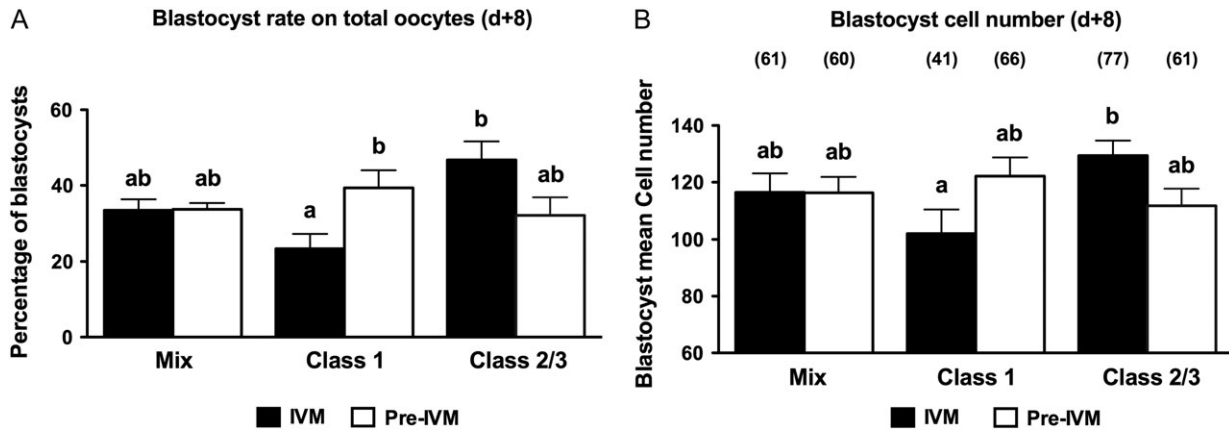


**Figure 7** Effect of pre-maturation treatment on COC with different morphology. After collection, COC were separated into Class 1 and Class 2/3 on the basis of their morphology and *in vitro* matured with or without the pre-IVM treatment. Then, oocytes were *in vitro* fertilized and *in vitro* cultured for 8 days. Groups of unsorted COC (mix of Class 1/2/3) were subjected to the same experimental procedure and were used as controls. Graphs show the effect of the pre-IVM treatment on the blastocyst rate (A) and mean cell number per blastocyst (B). A total of 947 oocytes were analyzed in this study (292 mixed oocytes, 321 Class 1 and 334 Class 2/3) in six independent experiments. Data were analyzed by one-way ANOVA followed by Newman–Keuls multiple comparison test; data are expressed as means  $\pm$  SEM; a, b: different letters indicates significant differences ( $P < 0.05$ ).

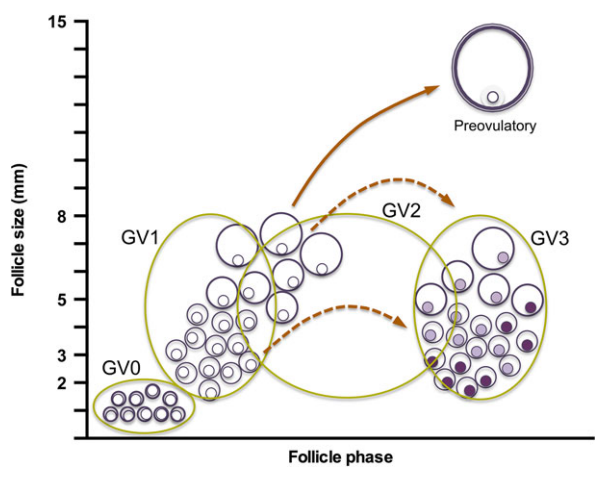


**Figure 8** Chromatin remodeling during follicular development: a model. The figure shows chromatin remodeling, as it would occur during the bovine estrous cycle. Follicles with white oocytes are non-atretic, while follicles with pink oocytes are early atretic and those with purple oocytes are atretic. The growing follicles would be mainly GV1, the plateau phase would be mainly GV2 and the early atretic would be GV3. Adapted from Merton et al. (2003).

and may induce endothelial cell apoptosis (Maisonpierre et al., 1997). In the cyclic ovary, ANGPT1, ANGPT2, Tie1 and Tie2, play important roles in the modulation of vascular growth and regression (Goede et al., 1998; Hazzard et al., 1999; Wulff et al., 2000, 2001a, b) and studies in cow revealed a function of this system in the remodeling of the vascular network specifically in the ovarian follicle (Hayashi et al., 2003, 2004). Strikingly, ANGPT2 was found to be upregulated in early atretic follicles (Hayashi et al., 2003; Girard et al., 2015), thus supporting our finding that CC\_GV3 are more prone to apoptosis.

These *in-silico* predictions are experimentally confirmed by the fact that the CC's susceptibility to apoptosis increases with oocyte's chromatin compaction. Moreover, these data are in agreement with previous findings indicating that functional gap junction-mediated communication between the oocyte and the surrounding CC is impaired in COC enclosing a GV3 oocyte and with signs of early cellular degeneration observed in GV3 oocytes at the ultrastructure level (Lodde et al., 2007, 2008). On the other hand, the present findings support the general idea that COC enclosing a GV1 oocyte are in an earlier stage of oocyte differentiation. In fact, Class 1 COC, which was originally characterized as the one with no morphological signs of degeneration and lower developmental competence (Blondin and Sirard, 1995; Hazeleger et al., 1995) and whose oocytes were found to be in an earlier stage of differentiation as assessed by BCB staining (present study), was the only class enriched in GV1 oocytes.

On the basis of our findings, we designed a tailored culture system, which confirmed that the success of *in vitro* cultural strategies aimed at improving oocyte developmental capability is 'stage dependent', i.e. mainly due to the characteristic of the COC that are subjected to the procedure. Indeed we demonstrated that standard IVM conditions are inappropriate to support pre-implantation embryonic development of GV1-enriched Class 1 COC, while their developmental competence is positively affected by a 6 h period of inhibition of meiotic resumption through cAMP modulators. On the contrary, the same treatment negatively affected Class 1 and 2 COC developmental competence, which is consistent with the findings that these classes only contain GV2 and GV3 oocytes. This in turn confirms earlier studies in which prolonged Pre-IVM (24 h) increased GV0 meiotic and developmental competencies (Luciano et al., 2011). These data are consistent with one of the concepts beyond pre-maturation strategies (Gilchrist, 2011; Sirard, 2011; Smitz et al., 2011; Franciosi et al., 2014; Gilchrist et al., 2016), i.e. the prolongation of GJ-mediated communication between the somatic and germinal compartments is expected to be more effective in COC with a functional oocyte-CC coupling (as in GV0 and GV1 (Lodde et al., 2007)).

An important finding of the present work is that, in naturally cycling animals, COC selection based on follicle size does not allow isolation of a homogeneous population in terms of chromatin configuration. This implies that at each follicular wave, GV1-to-GV2 transition, which marks the acquisition of a high embryonic developmental potential, occurs at almost any size as the growth of the follicle slows down before dominant follicle emergence and concomitantly with decline in the FSH level (Adams *et al.*, 2008; Forde *et al.*, 2011). After the highest FSH level is attained in the preovulatory peak, the atretic events would start and GV2-to-GV3 transition eventually occurs. The timing of such a sequence would fit the preparation of the oocyte for ovulation or atresia, which requires chromatin compaction in both cases. This further confirms a previously postulated hypothesis that 'GV3 oocytes represent that proportion of gametes, which have reached a high developmental capability during follicular growth, and that, at the time of collection, were undergoing early events of atresia' (Lodde *et al.*, 2007, 2008). These concepts are summarized in a tentative model illustrated in Fig. 8 which relates well with an average competence of 33% and early atresia improving developmental potential (Blondin and Sirard, 1995). If each follicle would contain a GV2 stage oocyte at its plateau phase and such status would be permissive for further development, it would explain the extraordinary stable blastocyst rate observed with bovine IVM since 1995. The growing follicles would be mainly GV1, the plateau phase would be (low FSH) GV2 and the early atretic would be GV3 with respectively low, high and medium developmental competence.

In conclusion, our data support the idea that the synchrony between nuclear, cytoplasmic and molecular events is finely tuned during the final phase of oocyte growth. Our results also demonstrate the necessity of a deep knowledge of the biological process occurring in CC during the final growth of the oocyte for the refinement of customized culture systems, which should consider the metabolic requirements of the heterogeneous population of oocytes that are submitted to IVM. This is mandatory to significantly improve assisted reproductive technologies. Very recently, a high similarity in the process of chromatin remodeling occurring in bovine and human immature oocytes, which reflects a high cellular and molecular heterogeneity in human oocytes, have been reported (Sanchez *et al.*, 2015). Thus, the present work may have important consequences for human IVM in which the results are still suboptimal compared to conventional IVF (Coticchio *et al.*, 2012). In addition to avoiding the primary adverse effects caused by ovarian stimulation, further improvements in IVM effectiveness and efficiency may help broaden the use of IVM for fertility preservation and in infertile patients.

## Supplementary data

Supplementary data are available at *Molecular Human Reproduction* online.

## Acknowledgements

The authors thank Dr Marina Perri of the Health Veterinary Inspection service at INALCA spa, and Drs Valentina Baruffini and Fabio Barbieri from University of Milan for technical support.

## Authors' roles

All authors contributed substantially to this manuscript. A.M.L., V.L. and M.A.S. designed the study; C.D., V.L., R.L., I.D., I.T. and A.M.L. executed experiments; C.D., R.L., V.L., A.M.L. and M.A.S. analyzed the data; V.L., C.D. and A.M.L. wrote the manuscript. All authors revised and approved the final manuscript.

## Funding

NSERC Strategic Network EmbryoGENE, Canada; CIG—Marie Curie Actions FP7-Reintegration-Grants within the 7th European Community Framework Programme (Contract: 303640, 'Pro-Ovum' to VL).

## Conflict of interest

None declared.

## References

- Aardema H, Lolicato F, van de Lest CH, Brouwers JF, Vaandrager AB, van Tol HT, Roelen BA, Vos PL, Helms JB, Gadella BM. Bovine cumulus cells protect maturing oocytes from increased fatty acid levels by massive intracellular lipid storage. *Biol Reprod* 2013;**88**:164.
- Adams GP, Jaiswal R, Singh J, Malhi P. Progress in understanding ovarian follicular dynamics in cattle. *Theriogenology* 2008;**69**:72–80.
- Albertini DF. Cytoplasmic microtubular dynamics and chromatin organization during mammalian oogenesis and oocyte maturation. *Mutat Res* 1992;**296**:57–68.
- Auclair S, Uzbekov R, Elis S, Sanchez L, Kireev I, Lardic L, Dalbies-Tran R, Uzbekova S. Absence of cumulus cells during in vitro maturation affects lipid metabolism in bovine oocytes. *Am J Physiol Endocrinol Metab* 2013;**304**:E599–613.
- Bernhardt ML, Kim AM, O'Halloran TV, Woodruff TK. Zinc requirement during meiosis I-meiosis II transition in mouse oocytes is independent of the MOS-MAPK pathway. *Biol Reprod* 2011;**84**:526–536.
- Bernhardt ML, Kong BY, Kim AM, O'Halloran TV, Woodruff TK. A zinc-dependent mechanism regulates meiotic progression in mammalian oocytes. *Biol Reprod* 2012;**86**:114.
- Blazejczyk M, Miron M, Nadon R. *FlexArray: A Statistical Data Analysis Software for Gene Expression Microarrays*. Montreal, Canada: Genome Quebec, 2007.
- Blondin P, Bousquet D, Twagiramungu H, Barnes F, Sirard MA. Manipulation of follicular development to produce developmentally competent bovine oocytes. *Biol Reprod* 2002;**66**:38–43.
- Blondin P, Sirard MA. Oocyte and follicular morphology as determining characteristics for developmental competence in bovine oocytes. *Mol Reprod Dev* 1995;**41**:54–62.
- Bonnet-Garnier A, Feuerstein P, Chebrou M, Fleuret R, Jan HU, Debey P, Beaujean N. Genome organization and epigenetic marks in mouse germinal vesicle oocytes. *Int J Dev Biol* 2012;**56**:877–887.
- Bouniol-Baly C, Hamraoui L, Guibert J, Beaujean N, Szollosi MS, Debey P. Differential transcriptional activity associated with chromatin configuration in fully grown mouse germinal vesicle oocytes. *Biol Reprod* 1999;**60**:580–587.
- Bunel A, Jorssen EP, Merckx E, Leroy JL, Bols PE, Sirard MA. Individual bovine in vitro embryo production and cumulus cell transcriptomic analysis to distinguish cumulus-oocyte complexes with high or low developmental potential. *Theriogenology* 2015;**83**:228–237.
- Bunel A, Nivet AL, Blondin P, Vigneault C, Richard FJ, Sirard MA. Cumulus cell gene expression associated with pre-ovulatory acquisition of

- developmental competence in bovine oocytes. *Reprod Fertil Dev* 2014; **26**:855–865.
- Coticchio G, Dal Canto M, Mignini Renzini M, Guglielmo MC, Brambillasca F, Turchi D, Novara PV, Fadini R. Oocyte maturation: gamete-somatic cells interactions, meiotic resumption, cytoskeletal dynamics and cytoplasmic reorganization. *Hum Reprod Update* 2015; **21**:427–454.
- Coticchio G, Dal-Canto M, Guglielmo MC, Mignini-Renzini M, Fadini R. Human oocyte maturation in vitro. *Int J Dev Biol* 2012; **56**:909–918.
- Culhane AC, Perriere G, Considine EC, Cotter TG, Higgins DG. Between-group analysis of microarray data. *Bioinformatics* 2002; **18**:1600–1608.
- De La Fuente R. Chromatin modifications in the germinal vesicle (GV) of mammalian oocytes. *Dev Biol* 2006; **292**:1–12.
- De La Fuente R, Eppig JJ. Transcriptional activity of the mouse oocyte genome: companion granulosa cells modulate transcription and chromatin remodeling. *Dev Biol* 2001; **229**:224–236.
- De La Fuente R, Viveiros MM, Burns KH, Adashi EY, Matzuk MM, Eppig JJ. Major chromatin remodeling in the germinal vesicle (GV) of mammalian oocytes is dispensable for global transcriptional silencing but required for centromeric heterochromatin function. *Dev Biol* 2004; **275**:447–458.
- Debey P, Szollosi MS, Szollosi D, Vautier D, Girousse A, Besombes D. Competent mouse oocytes isolated from antral follicles exhibit different chromatin organization and follow different maturation dynamics. *Mol Reprod Dev* 1993; **36**:59–74.
- Edgar R, Domrachev M, Lash AE. Gene Expression Omnibus: NCBI gene expression and hybridization array data repository. *Nucleic Acids Res* 2002; **30**:207–210.
- Eppig JJ. Oocyte control of ovarian follicular development and function in mammals. *Reproduction* 2001; **122**:829–838.
- Eppig JJ, Schultz RM, O'Brien M, Chesnel F. Relationship between the developmental programs controlling nuclear and cytoplasmic maturation of mouse oocytes. *Dev Biol* 1994; **164**:1–9.
- Forde N, Beltman ME, Lonergan P, Diskin M, Roche JF, Crowe MA. Oestrous cycles in *Bos taurus* cattle. *Anim Reprod Sci* 2011; **124**:163–169.
- Franciosi F, Coticchio G, Lodde V, Tessaro I, Modena SC, Fadini R, Dal Canto M, Renzini MM, Albertini DF, Luciano AM. Natriuretic peptide precursor C delays meiotic resumption and sustains gap junction-mediated communication in bovine cumulus-enclosed oocytes. *Biol Reprod* 2014; **91**:61.
- Gilbert I, Scantland S, Dufort I, Gordynska O, Labbe A, Sirard MA, Robert C. Real-time monitoring of aRNA production during T7 amplification to prevent the loss of sample representation during microarray hybridization sample preparation. *Nucleic Acids Res* 2009; **37**:e65.
- Gilbert I, Scantland S, Sylvestre EL, Dufort I, Sirard MA, Robert C. Providing a stable methodological basis for comparing transcript abundance of developing embryos using microarrays. *Mol Hum Reprod* 2010; **16**:601–616.
- Gilchrist RB. Recent insights into oocyte-follicle cell interactions provide opportunities for the development of new approaches to in vitro maturation. *Reprod Fertil Dev* 2011; **23**:23–31.
- Gilchrist RB, Lane M, Thompson JG. Oocyte-secreted factors: regulators of cumulus cell function and oocyte quality. *Hum Reprod Update* 2008; **14**:159–177.
- Gilchrist RB, Luciano AM, Richani D, Zeng HT, Wang X, Vos MD, Sugimura S, Smitz J, Richard FJ, Thompson JG. Oocyte maturation and quality: role of cyclic nucleotides. *Reproduction* 2016; **152**:R143–157.
- Girard A, Dufort I, Douville G, Sirard MA. Global gene expression in granulosa cells of growing, plateau and atretic dominant follicles in cattle. *Reprod Biol Endocrinol* 2015; **13**:17.
- Goede V, Schmidt T, Kimmina S, Kozian D, Augustin HG. Analysis of blood vessel maturation processes during cyclic ovarian angiogenesis. *Lab Invest* 1998; **78**:1385–1394.
- Gordon I. *Laboratory Production of Cattle Embryos*, 2nd edn. Cambridge MA (USA): CABI Publishing, 2003.
- Gougeon A. Dynamics of follicular growth in the human: a model from preliminary results. *Hum Reprod* 1986; **1**:81–87.
- Gougeon A. Regulation of ovarian follicular development in primates: facts and hypotheses. *Endocr Rev* 1996; **17**:121–155.
- Hayashi KG, Acosta TJ, Tetsuka M, Berisha B, Matsui M, Schams D, Ohtani M, Miyamoto A. Involvement of angiopoietin-tie system in bovine follicular development and atresia: messenger RNA expression in theca interna and effect on steroid secretion. *Biol Reprod* 2003; **69**:2078–2084.
- Hayashi KG, Berisha B, Matsui M, Schams D, Miyamoto A. Expression of mRNA for the angiopoietin-tie system in granulosa cells during follicular development in cows. *J Reprod Dev* 2004; **50**:477–480.
- Hazeleger NL, Hill DJ, Stubbing RB, Walton JS. Relationship of morphology and follicular fluid environment of bovine oocytes to their developmental potential in vitro. *Theriogenology* 1995; **43**:509–522.
- Hazzard TM, Molskness TA, Chaffin CL, Stouffer RL. Vascular endothelial growth factor (VEGF) and angiopoietin regulation by gonadotrophin and steroids in macaque granulosa cells during the peri-ovulatory interval. *Mol Hum Reprod* 1999; **5**:1115–1121.
- Hyttel P, Fair T, Callesen H, Greve T. Oocyte growth, capacitation and final maturation in cattle. *Theriogenology* 1997; **47**:23–32.
- Jolly PD, Tisdall DJ, Heath DA, Lun S, McNatty KP. Apoptosis in bovine granulosa cells in relation to steroid synthesis, cyclic adenosine 3',5'-monophosphate response to follicle-stimulating hormone and luteinizing hormone, and follicular atresia. *Biol Reprod* 1994; **51**:934–944.
- Kim AM, Bernhardt ML, Kong BY, Ahn RW, Vogt S, Woodruff TK, O'Halloran TV. Zinc sparks are triggered by fertilization and facilitate cell cycle resumption in mammalian eggs. *ACS Chem Biol* 2011; **6**:716–723.
- Kim AM, Vogt S, O'Halloran TV, Woodruff TK. Zinc availability regulates exit from meiosis in maturing mammalian oocytes. *Nat Chem Biol* 2010; **6**:674–681.
- Kim JY, Kinoshita M, Ohnishi M, Fukui Y. Lipid and fatty acid analysis of fresh and frozen-thawed immature and in vitro matured bovine oocytes. *Reproduction* 2001; **122**:131–138.
- Kong BY, Bernhardt ML, Kim AM, O'Halloran TV, Woodruff TK. Zinc maintains prophase I arrest in mouse oocytes through regulation of the MOS-MAPK pathway. *Biol Reprod* 2012; **87**:11–12.
- Kumar L, Futschik ME. Mfuzz: a software package for soft clustering of microarray data. *Bioinformatics* 2007; **23**:5–7.
- Labrecque R, Lodde V, Dieci C, Tessaro I, Luciano AM, Sirard MA. Chromatin remodeling and histone mRNA accumulation in bovine germinal vesicle oocytes. *Mol Reprod Dev* 2015; **82**:450–462.
- Landry DA, Bellefleur AM, Labrecque R, Grand FX, Vigneault C, Blondin P, Sirard MA. Effect of cow age on the in vitro developmental competence of oocytes obtained following FSH stimulation/coasting treatments. *Theriogenology* 2016; **86**:1240–1246.
- Lisle RS, Anthony K, Randall MA, Diaz FJ. Oocyte-cumulus cell interactions regulate free intracellular zinc in mouse oocytes. *Reproduction* 2013; **145**:381–390.
- Lodde V, Franciosi F, Tessaro I, Modena SC, Luciano AM. Role of gap junction-mediated communications in regulating large-scale chromatin configuration remodeling and embryonic developmental competence acquisition in fully grown bovine oocyte. *J Assist Reprod Genet* 2013; **30**:1219–1226.
- Lodde V, Modena S, Galbusera C, Franciosi F, Luciano AM. Large-scale chromatin remodeling in germinal vesicle bovine oocytes: interplay with gap junction functionality and developmental competence. *Mol Reprod Dev* 2007; **74**:740–749.
- Lodde V, Modena S, Maddox-Hyttel P, Franciosi F, Lauria A, Luciano AM. Oocyte morphology and transcriptional silencing in relation to

- chromatin remodeling during the final phases of bovine oocyte growth. *Mol Reprod Dev* 2008;**75**:915–924.
- Lodde V, Modina SC, Franciosi F, Zuccari E, Tessaro I, Luciano AM. Localization of DNA methyltransferase-I during oocyte differentiation, in vitro maturation and early embryonic development in cow. *Eur J Histochem* 2009;**53**:e24.
- Loneragan P, Fair T. In vitro-produced bovine embryos: dealing with the warts. *Theriogenology* 2008;**69**:17–22.
- Luciano AM, Franciosi F, Dieci C, Lodde V. Changes in large-scale chromatin structure and function during oogenesis: a journey in company with follicular cells. *Anim Reprod Sci* 2014;**149**:3–10.
- Luciano AM, Franciosi F, Modina SC, Lodde V. Gap junction-mediated communications regulate chromatin remodeling during bovine oocyte growth and differentiation through cAMP-dependent mechanism(s). *Biol Reprod* 2011;**85**:1252–1259.
- Luciano AM, Lodde V. Changes of large-scale chromatin configuration during mammalian oocyte differentiation. In: Cotichio G, Albertini DF, De Santis L (eds). *Oogenesis*. London: Springer, 2013:93–108.
- Luciano AM, Lodde V, Beretta MS, Colleoni S, Lauria A, Modina S. Developmental capability of denuded bovine oocyte in a co-culture system with intact cumulus-oocyte complexes: role of cumulus cells, cyclic adenosine 3',5'-monophosphate, and glutathione. *Mol Reprod Dev* 2005;**71**:389–397.
- Luciano AM, Modina S, Gandolfi F, Lauria A, Armstrong DT. Effect of cell-to-cell contact on in vitro deoxyribonucleic acid synthesis and apoptosis responses of bovine granulosa cells to insulin-like growth factor-I and epidermal growth factor. *Biol Reprod* 2000;**63**:1580–1585.
- Lussier JG, Matton P, Dufour JJ. Growth rates of follicles in the ovary of the cow. *J Reprod Fertil* 1987;**81**:301–307.
- Maisonpierre PC, Suri C, Jones PF, Bartunkova S, Wiegand SJ, Radziejewski C, Compton D, McClain J, Aldrich TH, Papadopoulos N et al. Angiopoietin-2, a natural antagonist for Tie2 that disrupts in vivo angiogenesis. *Science* 1997;**277**:55–60.
- Matorras R, Ruiz JJ, Mendoza R, Ruiz N, Sanjurjo P, Rodriguez-Escudero FJ. Fatty acid composition of fertilization-failed human oocytes. *Hum Reprod* 1998;**13**:2227–2230.
- Matzuk MM, Burns KH, Viveiros MM, Eppig JJ. Intercellular communication in the mammalian ovary: oocytes carry the conversation. *Science* 2002;**296**:2178–2180.
- Merton JS, de Roos AP, Mullaart E, de Ruigh L, Kaal L, Vos PL, Dieleman SJ. Factors affecting oocyte quality and quantity in commercial application of embryo technologies in the cattle breeding industry. *Theriogenology* 2003;**59**:651–674.
- Monniaux D, Clement F, Dalbies-Tran R, Estienne A, Fabre S, Mansanet C, Monget P. The ovarian reserve of primordial follicles and the dynamic reserve of antral growing follicles: what is the link? *Biol Reprod* 2014;**90**:85.
- Montani DA, Cordeiro FB, Regiani T, Victorino AB, Pilau EJ, Gozzo FC, Ferreira CR, Fraietta R, Lo Turco EG. The follicular microenvironment as a predictor of pregnancy: MALDI-TOF MS lipid profile in cumulus cells. *J Assist Reprod Genet* 2012;**29**:1289–1297.
- Nivet AL, Bunel A, Labrecque R, Belanger J, Vigneault C, Blondin P, Sirard MA. FSH withdrawal improves developmental competence of oocytes in the bovine model. *Reproduction* 2012;**143**:165–171.
- Pavlok A, Lucas-Hahn A, Niemann H. Fertilization and developmental competence of bovine oocytes derived from different categories of antral follicles. *Mol Reprod Dev* 1992;**31**:63–67.
- Robert C, Nieminen J, Dufort I, Gagne D, Grant JR, Cagnone G, Plourde D, Nivet AL, Fournier E, Paquet E et al. Combining resources to obtain a comprehensive survey of the bovine embryo transcriptome through deep sequencing and microarrays. *Mol Reprod Dev* 2011;**78**:651–664.
- Sanchez F, Romero S, De Vos M, Verheyen G, Smitz J. Human cumulus-enclosed germinal vesicle oocytes from early antral follicles reveal heterogeneous cellular and molecular features associated with in vitro maturation capacity. *Hum Reprod* 2015;**30**:1396–1409.
- Sirard MA. Follicle environment and quality of in vitro matured oocytes. *J Assist Reprod Genet* 2011;**28**:483–488.
- Smitz JE, Thompson JG, Gilchrist RB. The promise of in vitro maturation in assisted reproduction and fertility preservation. *Semin Reprod Med* 2011;**29**:24–37.
- Stringfellow DA, Givens MD. Manual of the International Embryo Transfer Society: A Procedural Guide and General Information for the Use of Embryo Transfer Technology Emphasizing Sanitary Procedures, 4th edn, IETS Publisher, Savoy, IL (USA), 2010.
- Su YQ, Sugiura K, Wigglesworth K, O'Brien MJ, Affourtit JP, Pangas SA, Matzuk MM, Eppig JJ. Oocyte regulation of metabolic cooperativity between mouse cumulus cells and oocytes: BMP15 and GDF9 control cholesterol biosynthesis in cumulus cells. *Development* 2008;**135**:111–121.
- Tian X, Anthony K, Neuberger T, Diaz FJ. Preconception zinc deficiency disrupts postimplantation fetal and placental development in mice. *Biol Reprod* 2014;**90**:83.
- Tian X, Diaz FJ. Zinc depletion causes multiple defects in ovarian function during the periovulatory period in mice. *Endocrinology* 2012;**153**:873–886.
- Tian X, Diaz FJ. Acute dietary zinc deficiency before conception compromises oocyte epigenetic programming and disrupts embryonic development. *Dev Biol* 2013;**376**:51–61.
- Tomer H, Ghanem N, Ambros C, Holker M, Tomek W, Phatsara C, Alm H, Sirard MA, Kanitz W, Schellander K et al. Molecular and subcellular characterisation of oocytes screened for their developmental competence based on glucose-6-phosphate dehydrogenase activity. *Reproduction* 2008;**135**:197–212.
- Vandesompele J, De Preter K, Pattyn F, Poppe B, Van Roy N, De Paepe A, Speleman F. Accurate normalization of real-time quantitative RT-PCR data by geometric averaging of multiple internal control genes. *Genome Biol* 2002;**3**:RESEARCH0034.
- Vassena R, Mapletoft RJ, Allodi S, Singh J, Adams GP. Morphology and developmental competence of bovine oocytes relative to follicular status. *Theriogenology* 2003;**60**:923–932.
- Vigone G, Merico V, Prigione A, Mulas F, Sacchi L, Gabetta M, Bellazzi R, Redi CA, Mazzini G, Adjaye J et al. Transcriptome based identification of mouse cumulus cell markers that predict the developmental competence of their enclosed antral oocytes. *BMC Genomics* 2013;**14**:380.
- Wang CY, Jenkitkasemwong S, Duarte S, Sparkman BK, Shawki A, Mackenzie B, Knutson MD. ZIP8 is an iron and zinc transporter whose cell-surface expression is up-regulated by cellular iron loading. *J Biol Chem* 2012;**287**:34032–34043.
- Wulff C, Wiegand SJ, Saunders PT, Scobie GA, Fraser HM. Angiogenesis during follicular development in the primate and its inhibition by treatment with truncated Flt-1-Fc (vascular endothelial growth factor Trap (A40)). *Endocrinology* 2001a;**142**:3244–3254.
- Wulff C, Wilson H, Lague P, Duncan WC, Armstrong DG, Fraser HM. Angiogenesis in the human corpus luteum: localization and changes in angiopoietins, tie-2, and vascular endothelial growth factor messenger ribonucleic acid. *J Clin Endocrinol Metab* 2000;**85**:4302–4309.
- Wulff C, Wilson H, Rudge JS, Wiegand SJ, Lunn SF, Fraser HM. Luteal angiogenesis: prevention and intervention by treatment with vascular endothelial growth factor trap(A40). *J Clin Endocrinol Metab* 2001b;**86**:3377–3386.
- Zuccotti M, Garagna S, Merico V, Monti M, Alberto Redi C. Chromatin organisation and nuclear architecture in growing mouse oocytes. *Mol Cell Endocrinol* 2005;**234**:11–17.
- Zuccotti M, Piccinelli A, Giorgi Rossi P, Garagna S, Redi CA. Chromatin organization during mouse oocyte growth. *Mol Reprod Dev* 1995;**41**:479–485.